Composites Part C: Open Access 2 (2020) 100014

Contents lists available at ScienceDirect

Composites Part C: Open Access

journal homepage: www.elsevier.com/locate/jcomc

Numerical analysis of the delamination in CFRP laminates: VCCT and XFEM assessment

S. Karmakov [a,b,*], F. Cepero-Mejías [b,c,d], J.L. Curiel-Sosa [b,c]

[a] Department of Aeronautics, Imperial College London, South Kensington Campus, Exhibition Road, London SW7 2AZ, United Kingdom
[b] Department of Mechanical Engineering, The University of Sheffield, Sir Frederick Mappin Building, Mappin Street, Sheffield S1 3JD, United Kingdom
[c] Computer-Aided Aerospace & Mechanical Engineering (CA2M) Research Group, Sir Frederick Mappin Building, Mappin Street, Sheffield S1 3JD, United Kingdom
[d] Industrial Doctorate Centre in Machining Science, The University of Sheffield, Sir Frederick Mappin Building, Mappin Street, Sheffield S1 3JD, United Kingdom

ARTICLE INFO

Keywords:
Delamination
VCCT
XFEM
Finite element
Modelling
Composites

ABSTRACT

This document develops a critical analysis of the capabilities offered by well-known numerical approaches such as eXtended Finite Element Method (XFEM) and Virtual Crack Closure Technique (VCCT) to predict delamination in composite materials. Despite several computational analyses having been performed so far, the study of the adequacy of using different modelling approaches in the delamination of composites is still limited. This paper addresses this matter, confronting the advantages and disadvantages offered by VCCT, a well-established numerical approach, and XFEM, a promising and relatively novel modelling technique. For this purpose, the delamination of carbon fibre reinforced polymer (CFRP) laminates is investigated with the simulation of three common tests: Double Cantilever Beam (DCB), End-Notch Flexure (ENF) and Mixed-Mode Bending (MMB). Numerical results are validated with experimental data, taken from other publications, for both modelling approaches analysed. Consistency is maintained for all finite element (FE) simulations carried out in this work to draw meaningful comparisons between XFEM and VCCT. Several interesting conclusions are extracted from this work. For instance, VCCT simulations overall have high accuracy and low computational time, while XFEM shows high capabilities to predict Mode I fracture.

1. Introduction

In the last decade, the use of polymer matrix composites (PMCs) components has been steadily increasing. This trend is motivated by their high strength-to-weight ratio, fatigue and corrosion resistance, or the excellent surface quality of their components [1,2]. All these excellent capabilities make composites an attractive solution to fulfil the strict demands in high performance applications. For instance, the aircraft Boeing 787 has achieved a 50% weigh fraction and 80% volume fraction on composites. As a result, 40.000–50.000 fasteners were removed and 1500 aluminium sheets were progressively replaced [3]. These changes allow for a considerable weight reduction and a notable enhancement in fuel efficiency in this aircraft model.

Generally, although composite parts are near net shape manufactured, machining operations such as drilling, milling or turning are required to accomplish the strict dimensional tolerances demanded. However, factors such as the presence of high abrasive fibres or tough resins lead to rapid tool wear, making PMCs materials difficult to machine [4]. As a result, several distinct failures such as sub-surface damage [5,6] or delamination [7] are usually obtained, decreasing the structural integrity of the final components. Delamination, which is commonly obtained through the generation of holes in drilling operations, is one of the most severe damages observed in PMCs, as it is demonstrated it has a high impact on the reduction of fatigue life and strength in parts [8]. Therefore, the study of crack propagation in this kind of failure becomes essential to guarantee the correct performance of the in-service parts.

Several experimental investigations have been successfully conducted to obtain interesting insights in the delamination of composites. For instance, Cepero et al. [9] compared different fracture toughness when crack propagation is parallel or perpendicular to the fibre orientation. This investigation concluded that crack propagation parallel to the fibre is more restrained due to the crack path generated requiring more energy to allow the advance of the crack tip. However, the high cost of composite materials and the equipment required in these trials reduce notably the information obtained using this methodology. FE analysis provides a virtual cost-effective solution for the analysis of

* Corresponding author at: Department of Aeronautics, Imperial College London, South Kensington Campus, Exhibition Road, SW7 2AZ London, United Kingdom.
E-mail addresses: karmakovst@gmail.com (S. Karmakov), fmcepero1@sheffield.ac.uk (F. Cepero-Mejías), j.curiel-sosa@sheffield.ac.uk (J.L. Curiel-Sosa).
URL: https://www.ms-idc.co.uk/meet-students (F. Cepero-Mejías), https://www.sheffield.ac.uk/mecheng/staff/jcurielsosa (J.L. Curiel-Sosa)

https://doi.org/10.1016/j.jcomc.2020.100014
Received 23 June 2020; Received in revised form 23 July 2020; Accepted 31 July 2020
Available online xxx

crack propagation, reducing the cost and time required in experimental processes.

The modelling approaches more commonly utilised to address this matter are the cohesive interface elements and VCCT. PMCs delamination has been widely studied, achieving excellent results in several studies. The most relevant investigations in this matter are conducted by Turon et al. [10,11] obtaining the formulations to calculate the interfacial strengths and maximum element size to guarantee an accurate numerical validation with experimental results. However, this methodology usually requires small element sizes to obtain accurate results with the consequent increase in the computational cost [12]. Therefore, despite the excellent results obtained using this modelling approach, the use of other numerical techniques which allow the use of coarser meshes in different fracture scenarios such as Mode I, Mixed mode and Mode II might be recommendable to reduce the computational cost.

VCCT is a method that has grown in popularity greatly, with numerous authors proposing enhanced approaches to deal with different scenarios. Shivakumar et al.[13] extended VCCT to the three-dimensional space. Xie and Biggers Jr.[14] used interface elements to calculate strain energy release rates, based on VCCT, of progressive crack growth in mixed-mode loading scenarios. Ricco et al. [15] introduce a new numerical procedure, based on VCCT, for the study of skin delamination in stiffened composite panels, subjected to compressive loads. De Carvalho et al.[16] combined the Floating Node Method with VCCT to accurately model delamination migrations in cross-ply laminates. Xie et al. [17] proposed a method, based on VCCT, for calculating the energy release rate for kinking cracks in a two-dimensional setting. Xie and Biggers Jr.[18,19] used interface elements based on VCCT to determine the direction of a changing delamination front, as well as to directly calculate the strain energy release rate.

XFEM is a relatively new and a promising method that was initially created for modelling discontinuities in isotropic materials, yet recent research has been focused around using it in new scenarios, such as for composites. Zhao et al. [20] used the XFEM method for single and multi-crack delamination scenarios in composites and intra and interlaminar crack propagation. Curiel-Sosa and Karapurath applied XFEM to predict delamination in GLARE under Mode I loading [21]. Bienias [22] combined XFEM and cohesive elements and explored the interaction between the matrix and the fibres in carbon/epoxy composites. Stazi et al. [23] and Laborde et al. [24] proposed methods for implementation of higher-order shape functions. Finally, Curiel-Sosa et al. [25] analysed the evolution of the energy release rate in a DCB test of a cross-ply laminate.

Despite several works having been successfully conducted so far using VCCT and XFEM on the study of composite delamination, to these authors' knowledge there are no publications analysing carefully the pros and cons of using the aforementioned modelling approaches. This article is focused on a critical investigation of the advantages and disadvantages of using VCCT and XFEM to predict composite delamination in different fracture scenarios. The paper layout is broken down as follows. Section 2 provides the mathematical insights of both modelling approaches addressed in this analysis. Subsequently, in Section 3 all the more relevant details of the FE model employed are explained. The analysis and discussion of the numerical results obtained is developed in Section 4. Finally, a summary with all important remarks extracted from this manuscript is provided in Section 5.

2. Mathematical insights

This section expands on the working principles of the VCCT and XFEM modelling approaches. The physical and mathematical models they are based on, as well as the fracture criteria adopted for the simulations are briefly described in the following lines.

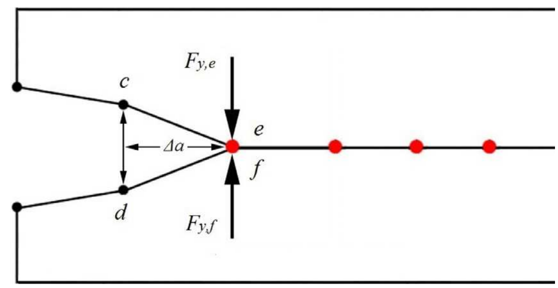

Fig. 1. VCCT method of debonding. The red and black nodes are constrained and debonded node-pairs, respectively.

2.1. VCCT method

Originally proposed by Rybicki and Kenninen [26], the VCCT method is based on the Linear Elastic Fracture Mechanics(LEFM) [27] and Irwin's criterion [28]. The underlying assumption behind the method is that the energy required to propagate a crack is the same as the energy required to close it to its original length. The equations for 4-noded elements are given in Eqs. (1) and (2). Raju [29] improved the model by adding higher-order interpolation elements, namely 8 and 12-noded elements. In general, the smaller the distance between neighbouring nodes, Δa, the more accurate Eqs. (1) and (2) will predict the strain energy release rate values.

$$G_I = \lim_{\Delta a \to 0} \frac{1}{2b\Delta a} F_y (v_c - v_d) \tag{1}$$

$$G_{II} = \lim_{\Delta a \to 0} \frac{1}{2b\Delta a} F_x (u_c - u_d) \tag{2}$$

The VCCT method simulates crack propagation and delamination by applying constraints to the nodes on the crack path. The nodes in front of the crack tip are coupled, to be released after the fracture criteria is met, simulating the advance of the crack [30], as shown in Fig. 1. VCCT requires a pre-defined crack path, which is restricted to the element boundaries [31]. As the model is governed by LEFM, before damage occurs, the system is linear-elastic. After the fracture criterion is reached, the constrained nodes become separated immediately without a damage evolution. The most common fracture criterion used in VCCT analyses is the BK-Law [32]. This criterion is based on the total energy release rate (G_T) and it is accomplished after the critical value (G_T^C) is reached, as it is illustrated in Eqs. (3) and (4).

$$f = \frac{G_T}{G_T^C} \tag{3}$$

where

$$G_T^C = G_I^C + (G_{II}^C - G_I^C)\left(\frac{G_{II}^C}{G_I^C + G_{II}^C}\right)^{\eta} \tag{4}$$

2.2. XFEM method

Initially proposed by Belytschko and Black [33], and then improved by Möes, Dolbow, and Belytschko[34], XFEM is based on Melenk and Babuška's [35] partition of unity property finite element method, which states that the sum of all shape functions is 1. The model provides additional degrees of freedom of the elements around the crack path and tip, allowing crack propagation through these meshed elements. The displacement functions, given in Eq. (5), allow the crack to propagate through these elements without constraints, or the need for remeshing. Thus XFEM is able to capture the crack opening and propagation as accurately as a standard FEA with very fine mesh would [36].

$$u = \sum_{I=1}^{S_I} N_I(x) u_I + \sum_{c=1}^{S_c} N_c(x) H(x) a_c + \sum_{t=1}^{S_t} N_t(x) \sum_{\alpha=1}^{4} F_\alpha(r,\omega) b_t^\alpha \tag{5}$$

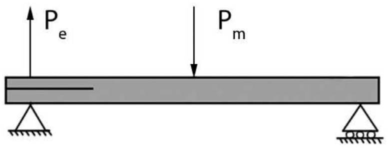

Fig. 2. Specimen boundary conditions

Table 1
Set-up parameters.

G_{II}/G_T	0%(*DCB*)	80%(*MMB*)	100%(*ENF*)
$a_0(mm)$	32.9	31.4	39.2
P_m	0	1.557P	P
P_e	P	0.558P	$P/4$

where S_I is the number of nodes of the elements containing the crack, S_c is the number of nodes of the elements containing the crack line, and S_t is the number of nodes of the elements containing the crack tip. N_I, N_c and N_t denote the respective shape functions of the nodes and u_I is the standard nodal displacement of node I. a_c and b_t are the nodal enriched degrees of freedom coefficients for the nodes of the elements containing the crack line and the crack tip, $H(x)$ is the Heaviside function, which generate the discontinuity through the elements to create the crack. F_α, the asymptotic enrichment function, adds degrees of freedom to the nodes of the element containing the crack tip, allowing the crack to grow.

$$F_\alpha(r,\omega) = \left\{ \sqrt{r}\cos\frac{\omega}{2}, \sqrt{r}\sin\frac{\omega}{2}, \sqrt{r}\sin\frac{\omega}{2}\sin\omega, \sqrt{r}\cos\frac{\omega}{2}\sin\omega \right\} \tag{6}$$

r and ω are the distance and angle of the crack inside the element with the crack tip. α is the number of nodes in the crack tip element. The XFEM model also follows LEFM, until the start of the crack propagation, but unlike VCCT, XFEM follows a damage evolution region. The failure criterion used in this paper to determine damage initiation is the quadratic traction criterion, or QUADS[37].

$$\left(\frac{\langle t_n \rangle}{t_n^0}\right)^2 + \left(\frac{t_s}{t_s^0}\right)^2 + \left(\frac{t_t}{t_t^0}\right)^2 = 1 \tag{7}$$

t_n, t_s and t_t are the nominal normal, shear and transverse tranctions, with t_n^0, t_s^0 and t_t^0 being the respective peak values. When this failure criterion is achieved, a linear energy-based softening controlled by the BK-Law is applied; it is chosen in order to keep the consistency with the VCCT simulations. Finally, once the critical strain energy release rate (G_T^C), defined in Eq. (4) is accomplished, the crack propagates through the element.

3. Finite element model characteristics

This paper uses Reeder and Crews' mixed-mode delamination test method and experimental data [38,39] to verify the performance of the two methods. By adjusting only the length of the loading lever, any MMB loading scenario is achieved, without changing the test configuration. Camanho et al. [40] and Turon and Camanho [10,41] used this test method and Reeder and Crews' experimental data as verification for their simulations. For both methods, the simulations are conducted as closely as possible to the tests in the original papers to keep the consistency and ensure the accuracy of the numerical results.

Three tests are conducted to compare the accuracy and effectiveness of the two methods: DCB, ENF and MMB. The loading and boundary conditions are presented in Fig. 2 and the set-up parameters for each test investigated are presented in Table 1. The simulated specimen consists of two parts, each 102mm long, 1.56mm thick and 25.4mm wide. The bottom ply is constrained at its ends with a pin and a roller support. The edge force P_e is applied at the end of the top ply, from the side of the pin support ($U_x = U_y = 0$). a_0 represents the distance between the middle force P_m and P_e; this distance is modified by the type of test conducted. The material used is AS4/PEEK carbon-reinforced polymer, with material properties listed in Table 2.

Due to the nature of the XFEM method, the XFEM crack must pass through some of the specimen's elements. Thus, in order to define an XFEM crack in the interface between the two specimen plies, a thin 0.01 mm layer of PEEK is inserted in the interface between the two plies. The initial crack is allocated in the middle of this layer with the dimensions specified in Table 1 for each test. It was assumed that the interlaminar crack would travel in the resin-rich region between the plies. Delamination cracks occur in the interlaminar region, which comprises of epoxy resin. Thus in order to more accurately simulate the real mechanism of delamination, this layer was added with the intention of creating a medium for the XFEM crack to propagate. Due to the small thickness of this layer, its addition has an insignificant effect on the results.

In this work, 4-noded CPE4R plane strain meshed elements available in Abaqus/Implicit are used in all simulations. Several meshes with different element sizes are modelled here to guarantee the accuracy of the results is not dependant of the element size. For VCCT, a local mesh refinement around the crack tip is conducted, as this is considered to be the most critical region of interest. The boundary conditions implemented for both tests were very restrictive. This, in combination with the complexity added by the anisotropic nature of composite materials, made the XFEM convergence challenging. Simulations with course meshes failed to converge. To aid the convergence, mesh refinement was implemented in the thin interface layer, resulting in very slender interface elements. To keep the aspect ratio of these elements reasonable, a further mesh refinement was required. As the interface and ply layers share the same nodes, this resulted in a mesh refinement in the plies as well. Different local mesh refinements were tested, yet they either did not converge, or produced inaccurate results. A global mesh refinement is implemented, as it allows the model to converge and to accurately simulate the crack propagation.

4. Analysis and discussion of numerical results

This section introduces and conducts an analysis on the results obtained from the Finite Element simulations developed in this investigation. For each test, the obtained results are presented as follows. Two side-by-side graphs present the convergence studies done for VCCT (left graph) and XFEM (right graph), for the given test set-up. This is followed by a graph with the converged results from each of the two methods. The final figure in each test subsection is a close-up view of the maximum principle stresses at the specimen crack tip at the moment of crack onset. For all graphs, the experimental results from Reeder and Crews[38,39] are included for verification of the accuracy of the results. The subsections with results are followed by a overall analysis and discussion subsection.

4.1. DCB results

The VCCT model predicts the linear region, before the crack propagation, very accurately for all the tested element sizes, with the 0.1 mm element size simulation capturing the overall shape the best. It is observed that the mesh refinement does not significantly contribute to the accuracy of the simulation after the damage initiation. For the XFEM simulation, the results do not show a good correlation with the experimental data for large element sizes; substantial improvement is observed in the accuracy of the predictions with the refinement of the mesh.

In both models, the linear and non-linear regions are predicted very accurately with the smallest element size of 0.1 mm, see Fig. 3. XFEM performs visibly better than VCCT in simulations with small element sizes. The curve of the XFEM results lacks the spiked behavior, present in the VCCT simulation, thus XFEM maps the experimental data more accurately. This is observed due to XFEM using a smaller increment of

Table 2
Material properties of AS4/PEEK.

E_{11}	$E_{22} = E_{33}$	$G_{12} = G_{13}$	G_{23}	$\upsilon_{12} = \upsilon_{12}$	ν_{23}
122.7 GPa	10.1 GPa	5.5 GPa	3.7 GPa	0.25	0.45
G_I^C	G_{II}^C	G_{III}^C	N	S_1	S_2
0.969 N/mm	1.719 N/mm	1.719 N/mm	80 MPa	100 MPa	100 MPa

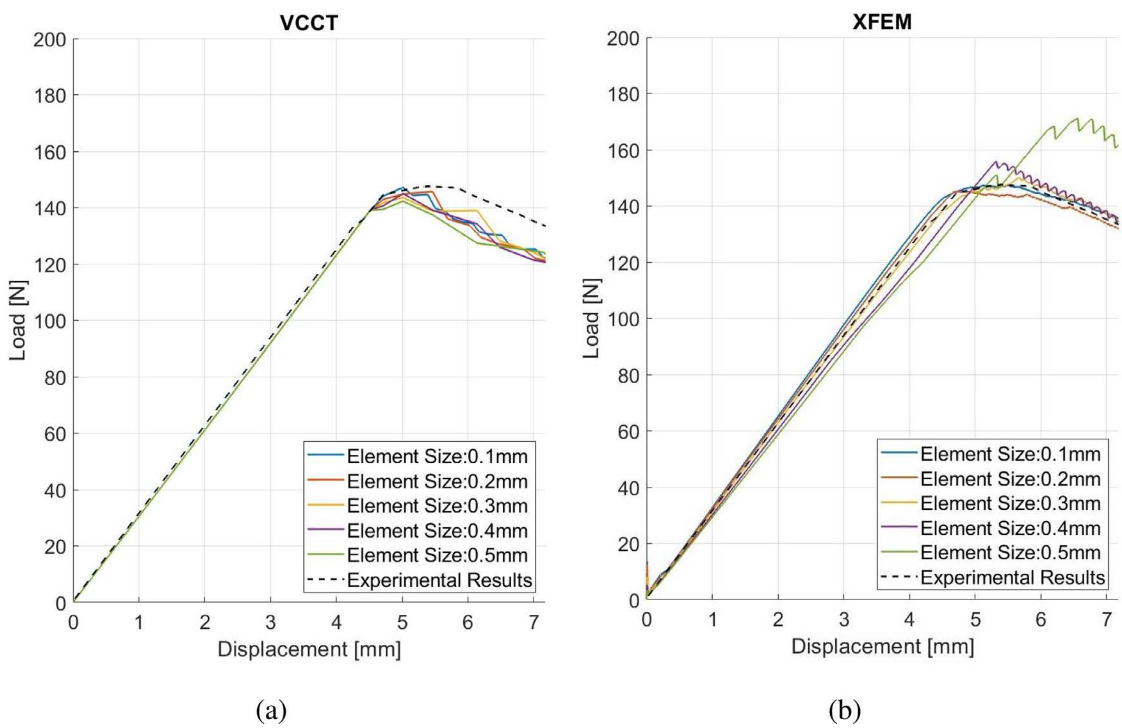

Fig. 3. Convergence study of VCCT and XFEM models for DCB test configuration.

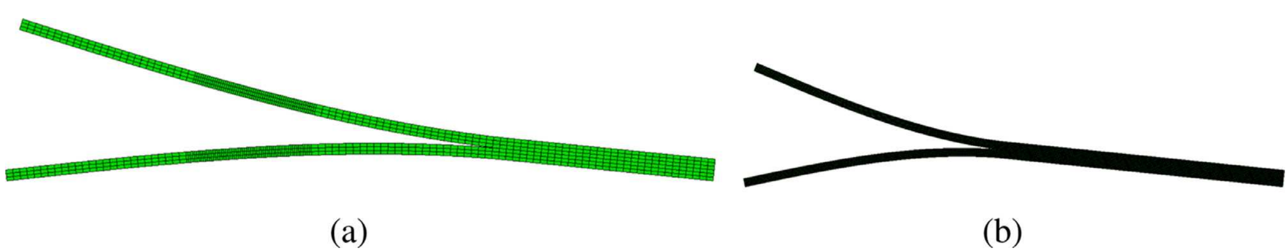

Fig. 4. Representation of the final deformed configuration for DCB simulations with and element size of 0.1mm for both FE investigated models: (a) VCCT and (b) XFEM.

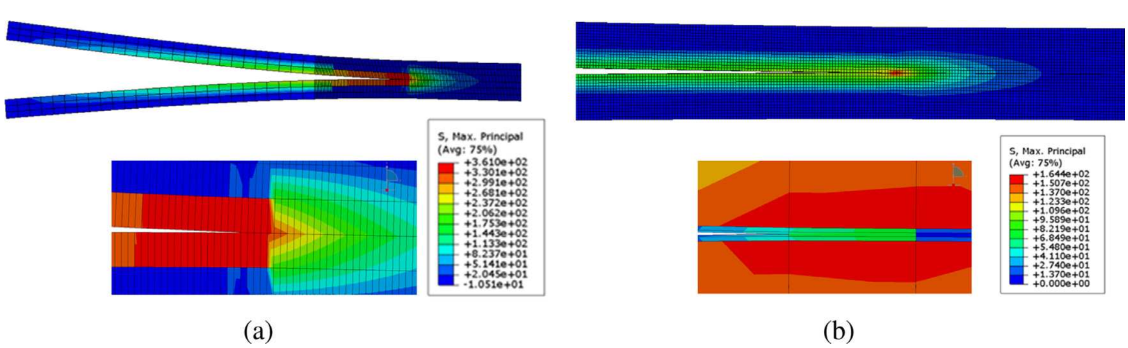

Fig. 5. Close-up view of the crack tip and the mesh of the simulated specimen at the first step after the crack onset, for both FE models: (a) VCCT and (b) XFEM. The mesh size is the same as for the respective models in Fig. 4: 0.1mm. The color map gives information about the maximum principle stresses.

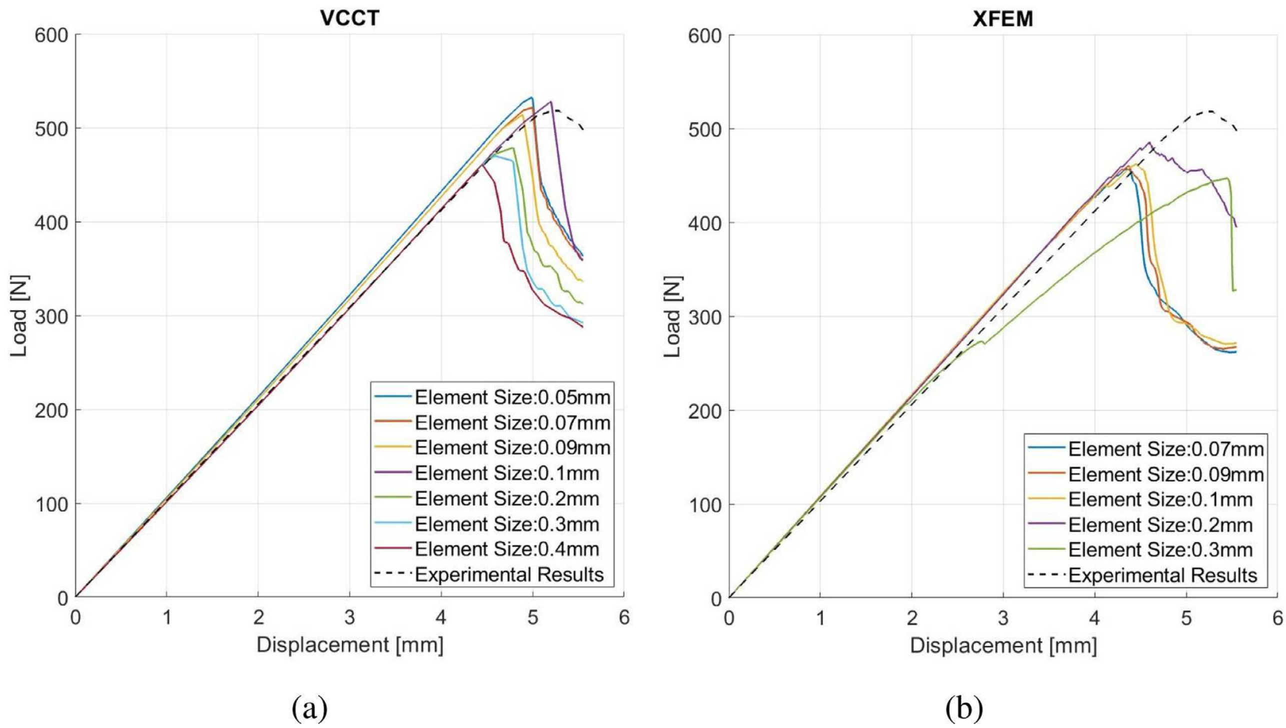

Fig. 6. Convergence study of VCCT and XFEM models for MMB test configuration.

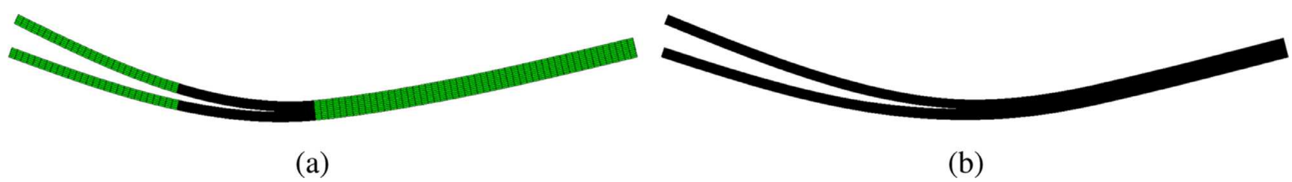

Fig. 7. Representation of the final deformed configuration for MMB simulations with and element size of 0.05mm and 0.07mm respectively for the two FE investigated models: (a) VCCT and (b) XFEM.

the time step to reach convergence, in comparison with the VCCT simulations. A representation of the final simulation results for both FE investigated models is provided in Fig. 4.

4.2. MMB results

The VCCT model requires greater element size refinement until it reaches convergence. With an element size of 0.1 mm, the results match the experimental data well; however, further refinement yields different results, thus the mesh convergence study is continued until convergence is reached with an element size of 0.05 mm. Despite the VCCT model accurately predicting the linear region, after the start of the crack propagation, the curve dips fast, exhibiting brittle crack growth and failing to properly map the non-linear region, as illustrated in Fig. 6(a).

The XFEM method reaches convergence at a smaller element size, compared to the DCB test, yet it fails to accurately predict both the linear region and the specimen behavior after the crack onset. Both the end and middle loadings created tensile stresses on the bottom part of the upper ply. Due to the asymmetric nature of the applied loading, the stresses at the crack tip did not point parallel to the interlaminar layer, but towards the upper ply, see Fig. 8(b). The crack, propagating in the direction of the highest stresses, escaped from the interlaminar layer and entered the upper ply, becoming an intralaminar crack. This changed the medium in which it propagated, leading to the crack propagating at a lower crack opening, and thus loading, than experimentally observed.

The crack migration that occurred in the XFEM simulations is a result of the XFEM model not pre-defining the crack path. For the VCCT model, the crack path is mapped before the start of the simulation, thus even if the highest stresses pointed in a different direction, the crack would propagate along the pre-defined path. In order to correct this crack behaviour for the XFEM simulations, two numerical treatments are tested. The longitudinal modulus of elasticity of the interlaminar layer is decreased with the intent of making the region more favourable for crack onset. The fracture criteria from the upper and lower plies are removed to force the crack to propagate only inside the interlaminar region. Both methods are unsuccessful. It is considered that the initial assumption of making the interlaminar layer 0.01 mm thick may have been too conservative. A thicker layer could have been able to contain the crack within its boundaries. This is a numerical problem with the XFEM simulations, caused by the initial assumptions and conditions used.

4.3. ENF results

The VCCT model reaches convergence fast. Even though convergence was reached at an element size of 0.2 mm, the results from the simulation with 0.3 mm element size are the most accurate, predicting the linear region and the beginning of the crack propagation almost exactly. For the XFEM method, convergence is considered reached at 0.1 mm element size, even though the most accurate simulation is reached with 0.2 mm mesh size, as shown in Fig. 9. For both methods, the simulations that produce the best results and the simulations for which convergence was reached do not coincide, but are very close in terms of element size. The modelling of the composite plies relies on the assumption that the fibers are perfectly uniformly distributed in the

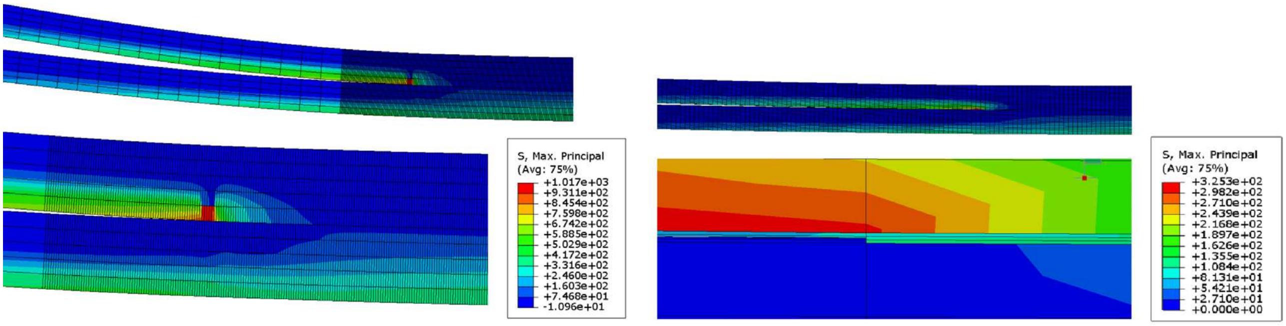

(a) (b)

Fig. 8. Close-up view of the crack tip and the mesh of the simulated specimen at the first step after the crack onset, for both FE models: (a) VCCT and (b) XFEM. The mesh size is the same as for the respective models in Fig. 7: 0.05 mm and 0.07 mm.The color map gives information about the maximum principle stresses.

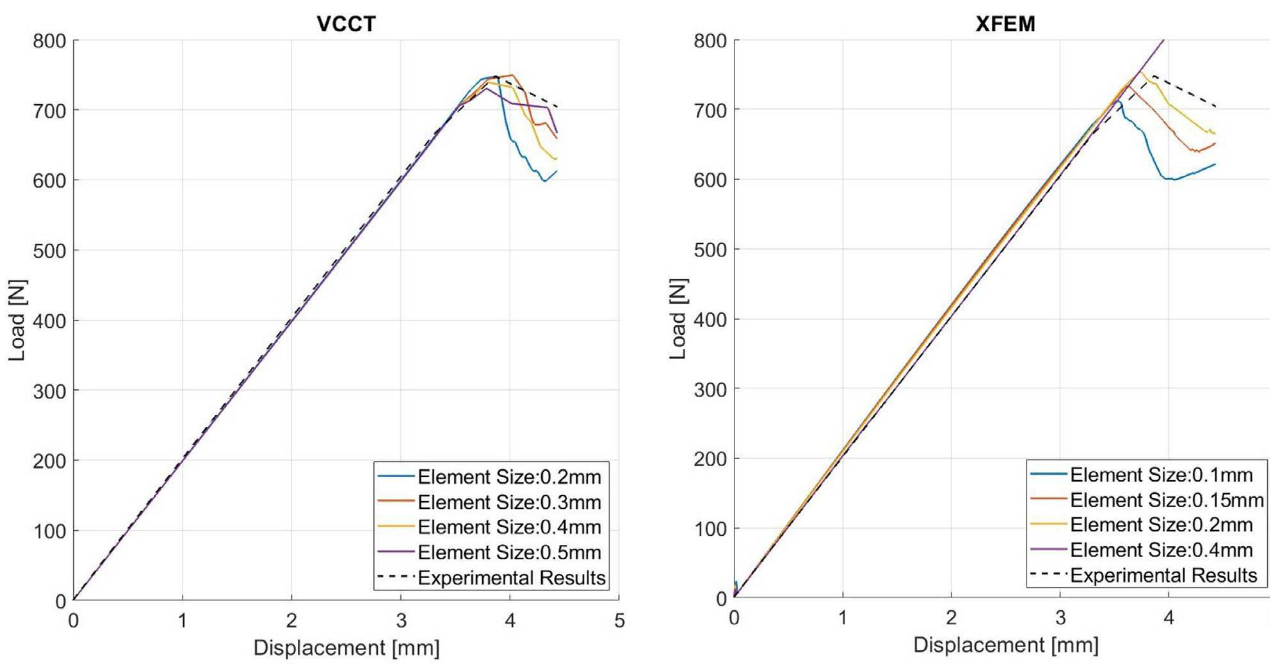

(a) (b)

Fig. 9. Convergence study of VCCT and XFEM models for ENF test configuration.

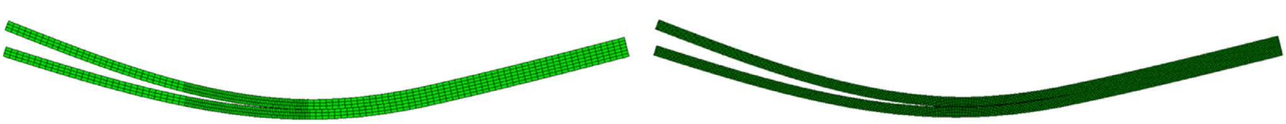

(a) (b)

Fig. 10. Representation of the final deformed configuration for ENF simulations with and element size of 0.3 mm and 0.2 mm respectively for the two FE investigated models: (a) VCCT and (b) XFEM.

matrix. This assumption brings some uncertainty into the simulations, which was considered enough to change the convergence element size values by 0.1 mm. Thus, it was taken that for both methods the most accurate simulation values are representative.

Just like with the MMB tests, the XFEM model suffers from crack migration from the inter-laminar layer into the upper ply. The lower end-loading for the ENF tests (in comparison with the MMB tests) results in the tensile stresses at the crack tip being lower and having a smaller vertical component, see Fig. 11(b). Consequently, the crack does not propagate deep into the ply, but stays close to the interface layer. The loading scenario also causes the excessive specimen central deflection, as shown on Fig. 10(b). Still this deflection is lower than the one observed for the MMB test, in Fig. 7(b), shedding further light into why the ENF crack migration was not as severe. This leads to the obtained results being closer to the experimental values (in comparison with the MMB simulations). Yet as crack migration is still present, the results fall short of accurately mapping the curve properly.

4.4. Numerical accuracy and computational cost discussion

The error between the predicted load for delamination crack initiation and the experimental values for each of the tests is presented in

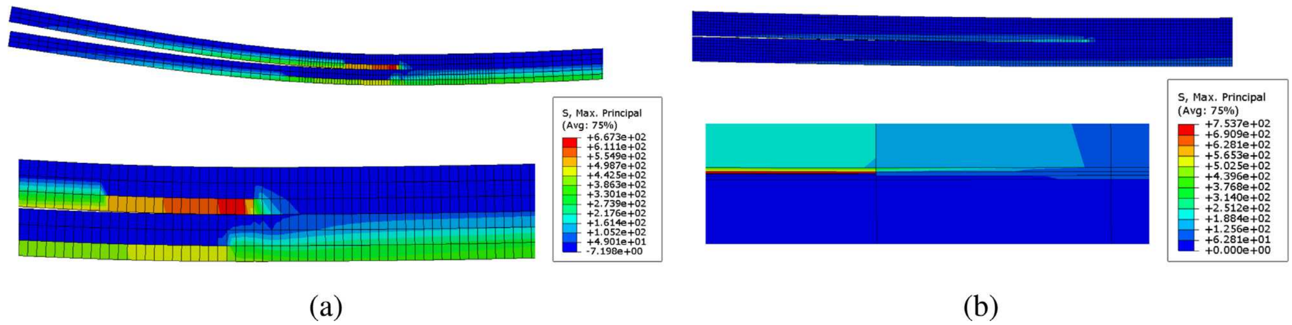

Fig. 11. Close-up view of the crack tip and the mesh of the simulated specimen at the first step after the crack onset, for both FE models: (a) VCCT and (b) XFEM. The mesh size is the same as for the respective models in Fig. 10: 0.3 mm and 0.2 mm. The color map gives information about the maximum principle stresses.

Table 3
Load required for crack onset error.

	DCB	*MMB*	*ENF*
VCCT	0.3%	1.12%	0.5%
XFEM	1.11%	13.2%	4.8%

Table 4
Largest simulation times for every test modelled in this work.

	DCB	*MMB*	*ENF*
VCCT	337s	1574s	152s
XFEM	16580s	32070s	28321s

Table 3. For the DCB and ENF tests, the VCCT model predicted the linear region, before the crack propagation, very accurately. The predicted crack initiation load is within less than a percent of the experimental values, further demonstrating the high accuracy of the DCB and ENF models' predictive capabilities. The accuracy of the predictions for the non-linear region are close to the experimental data, yet the accuracy deteriorates as the delamination progresses. The XFEM model predicts the delamination crack initiation worse for all tests. For the MMB and ENF tests, this is a direct cause of the crack migration problem. For the DCB test however, the slightly higher error for the crack onset (compared to the VCCT model) is compensated by a much better agreement with the experimental results for the rest of the curve. This is especially true in the non-linear region, where all other tests failed to produce accurate results.

All the simulations are developed in a computer with access to 8 virtual cores, 8GB of RAM and 1GB of VRAM. Interesting conclusions of the computational cost of every numerical test assessed are extracted from Table 4, where all the longest simulation times obtained in this work are showcased. These conclusions are broken down in the following lines. The VCCT model has short simulation times, even with very small mesh sizes. The MMB test simulation is significantly slower, compared to the other two, as previously discussed due to the more complicated stress distribution in the specimen, requiring a much finer mesh to reach convergence.

The computational cost of the simulations developed using XFEM is significantly higher in comparison with the VCCT. This occurs due to the use of a global mesh refinement to achieve the convergence of the simulation, which significantly increase the mesh elements. A glance to Table 4 reveals that MMB and ENF simulation times are significantly higher than the DCB ones. The explanation of this is that the observed ply migration of the crack in the MMB and ENF simulations adds several problems, making convergence harder. These problems are reduced with the use of smaller element sizes. Between the MMB and ENF tests, the MMB simulations are computationally heavier due to the larger number of elements required to reach convergence.

5. Conclusions

This paper has developed an exhausting analysis of the capabilities of the well-known VCCT modelling approach and the promising and relatively novel numerical technique, XFEM, to model composite delamination. For this purpose, thee different crack scenarios such as DCB, MMB and ENF tests have been successfully modelled. A different mesh is selected for each FE model in order to address the convergence requirements to obtain good numerical accuracy. Interesting insights extracted from this investigation are broken down below.

- VCCT is proved to predict better the crack onset in all the studied scenarios.
- Mode I fracture (DCB problem) is observed to be simulated more faithfully using XFEM.
- MMB and ENF tests are predicted with a higher accuracy using VCCT.
- Convergence problems are detected in XFEM simulations, which require the use of a fine mesh to obtain conclusive results. This contrasts with the coarser mesh employed in VCCT simulations, without a reduction in numerical accuracy.
- Computational cost is considerably higher in XFEM simulations in comparison with the time required in VCCT FE models.
- Crack migration problems have been found in the simulation of the MMB and ENF tests using XFEM because the large central specimen deflection introduces numerical errors in the crack path; this happens because the maximum stress does not follow exactly the correct crack path. This problem is reduced with the longitudinal stiffness reduction in the region where the crack propagates.

Considering the aforementioned statements, it could be concluded that VCCT offers better capabilities in general to predict composite delamination. Numerical convergence problems should be addressed in the future for the current numerical software to allow a promising modelling technique like XFEM to achieve better effectiveness in the prediction of composite delamination.

Declaration of Competing Interest

The authors whose names are listed immediately below certify that they have NO affiliations with or involvement in any organization or entity with any financial interest (such as honoraria; educational grants; participation in speakers' bureaus; membership, employment, consultancies, stock ownership, or other equity interest; and expert testimony or patent-licensing arrangements), or non-financial interest (such as personal or professional relationships, affiliations, knowledge or beliefs) in the subject matter or materials discussed in this manuscript.

The authors whose names are listed immediately below report the following details of affiliation or involvement in an organization or entity with a financial or non-financial interest in the subject matter or materials discussed in this manuscript. Please specify the nature of the conflict on a separate sheet of paper if the space below is inadequate.

Acknowledgements

The third author would like to acknowledge the financial support (EP/L016257/1) and technical help provided by the Industrial Doctoral Centre (IDC) of Sheffield and the Engineering and Physical Sciences Research Council (EPSRC).

References

[1] J.C. Halpin, Primer on Composite Materials Analysis, second ed., Revised, CRC Press, 1992.
[2] C. Soutis, Fibre reinforced composites in aircraft construction, Prog. Aerosp. Sci. 41 (2005) 143–151.
[3] Boeing, Boeing 787 Dreamliner, 2019.
[4] K. Kerrigan, G. Donnell, On the relationship between cutting temperature and workpiece polymer degradation during CFRP edge trimming, Procedia CIRP 55 (2016) 170–175.
[5] F. Cepero-Mejias, V. Phadnis, J. Curiel-Sosa, Machining induced damage in orthogonal cutting of UD composites: FEA Machining induced damage in orthogonal cutting of UD composites: FEA based assessment of Hashin and Puck criteria, in: 17th CIRP Conf. Model. Mach. Oper., 82, 2019, pp. 332–337.
[6] F. Cepero-Mejías, J. Curiel-Sosa, C. Zhang, V. Phadnis, Effect of cutter geometry on machining induced damage in orthogonal cutting of UD polymer composites: FE study, Compos. Struct. 214 (February) (2019) 439–450.
[7] V. Phadnis, F. Makhdum, A. Roy, V. Silberschmidt, Drilling in carbon / epoxy composites: experimental investigations and finite element implementation, Compos. Part A Appl. Sci. Manuf. 47 (2013) 41–51.
[8] E. Persson, I. Eriksson, L. Zackrisson, Effects of hole machining defects on strength and fatigue life of composite laminates, Compos. Part A Appl. Sci. Manuf. 28 (1997) 141–151.
[9] F. Cepero, I.G. García, J. Justo, V. Mantič, F. París, An experimental study of the translaminar fracture toughnesses in composites for different crack growth directions, parallel and transverse to the fiber direction, Compos. Sci. Technol. 181 (February) (2019) 1076–1079.
[10] A. Turon, P. Camanho, J. Costa, J. Renart, Accurate simulation of delamination growth under mixed-mode loading using cohesive elements: definition of interlaminar strengths and elastic stiffness, Compos. Struct. 92 (2010) 1857–1864.
[11] A. Turon, C. Dávila, P. Camanho, J. Costa, An engineering solution for mesh size effects in the simulation of delamination using cohesive zone models, Eng. Fract. Mech. 74 (10) (2007) 1665–1682.
[12] K. Song, C. Davila, C. Rose, Guidelines and parameter selection for the simulation of progressive delamination, in: 2008 ABAQUS User's Conf., 2008, pp. 1–15.
[13] K. Shivakumar, P. Tan, J. Newman, Virtual crack closure technique for calculating stress-intensity factors for cracked three-dimensional bodies, International Journal of Fracture 36 (1988) 43–50.
[14] D. Xie, S. Biggers Jr., Progressive crack growth analysis using interface element based on the virtual crack closure technique, Finite Elem. Anal. Des. 42 (2006) 977–984.
[15] A. Ricco, A. Raimondo, F. Scaramuzzino, A study on skin delaminations growth in stiffened composite panels by a novel numerical approach, Appl. Compos. Mater. 20 (2012) 465–488.
[16] N. De Carvalho, B. Chen, S. Pinho, J. Ratcliffe, P. Baiz, T. Tay, Modeling delamination migration in cross-ply tape laminates, Compos. Part A 71 (2015) 465–488.
[17] D. Xie, A. Waas, K. Shahwan, J. Schroeder, R. Boeman, Computation of energy release rates for kinking cracks based on virtual crack closure technique, CMES 6 (2004) 515–524.
[18] D. Xie, S. Biggers Jr., Strain energy release rate calculation for a moving delamination front of arbitrary shape based on the virtual crack closure technique. Part I: formulation and validation, Eng. Fract. Mech. 73 (2006) 771–785.
[19] D. Xie, S. Biggers Jr., Strain energy release rate calculation for a moving delamination front of arbitrary shape based on the virtual crack closure technique. Part II: sensitivity study on modeling details, Eng. Fract. Mech. 73 (2006) 786–801.
[20] L. Zhao, J. Zhi, J. Zhang, Z. Liu, N. Hu, XFEM simulation of delamination in composite laminates, Compos. Part A 80 (2016) 61–71.
[21] N. Curiel Sosa, J.L. Karapurath, Delamination modelling of GLARE using the extended finite element method, Compos. Sci. Technol. 72 (2012) 788–791.
[22] J. Bienias, H. Debski, B. Surowska, T. Sadowski, Analysis of microstructure damage in carbon/epoxy composites using FEM, Comput. Mater. Sci. 64 (2012) 168–172.
[23] F.L. Stazi, E. Budyn, J. Chessa, T. Belytschko, An extended finite element method with higher-order elements for curved cracks, Comput. Mech. 31 (2003) 38–48.
[24] P. Laborde, J. Pommier, Y. Renard, M. Salaün, High-order extended finite element method for cracked domains, Int. J. Numer. Methods Eng. 64 (2005) 354–381.
[25] J.L. Curiel Sosa, B. Tafazzolimoghaddam, C. Zhan, Modelling fracture and delamination in composite laminates: energy release rate and interface stress, Compos. Struct. 64 (2018) 641–647.
[26] E.F. Rybicki, M.F. Kanninen, A finite element calculation of stress intensity factors by a modified crack closure integral, Eng. Fract. Mech. 9 (1977) 931–938.
[27] M. Janssen, J. Zuidema, R. Wanhill, Fracture Mechanics, Spon Press, Abingdon, 2004.
[28] G. Irwin, Analysis of stresses and strains near the end of a crack traversing a plate, J. Appl. Mech. 24 (1957) 361–364.
[29] I.S. Raju, Calculation of strain-energy release rates with higher order and singular finite elements, Eng. Fract. Mech. 28 (1987) 251–274.
[30] ABAQUS, Abaqus Analysis User's Manual.
[31] R. Krueger, Virtual Crack Closure Technique: History, Approach, and Applications, Technical Report, 2002, doi:10.1115/1.1595677.
[32] M. Benzeggagh, M. Kenane, Measurement of mixed-mode delamination fracture toughness of unidirectional glass/epoxy composites with mixed-mode bending apparatus, Compos. Sci. Technol. 56 (1996) 439–449.
[33] T. Belytschko, T. Black, Elastic Crack Growth in finite elements with minimal remeshing, Int. J. Numer. MethodsEng. 45 (1999) 601–620, doi:10.3760/cma.j.issn.0366-6999.2011.18.023.
[34] N. Moës, J. Dolbow, T. Belytschko, A finite element method for crack growth without remeshing, Int. J. Numer. MethodsEng. 46 (1999) 131–150.
[35] J.M. Melenk, I. Babuška, The partition of unity finite element method: basic theory and applications, Comput. Methods Appl. Mech.Eng. 139 (1–4) (1996) 289–314, doi:10.1016/S0045-7825(96)01087-0.
[36] A. Khoei, Extended Finite Element Method: Theory and Applications, First Edition, John Witley \& Sons Ltd., 2015.
[37] ABAQUS, Abaqus Analysis User's Guide.
[38] J. CrewsJr, J. Reeder, A Mixed-mode Bending Apparatus for Delamination Testing, Technical Report, 1988.
[39] J. Reeder, J. Crews Jr, Mixed-mode bending method for delamination testing, AIAA J. 28 (1990) 1270–1276.
[40] P. Camanho, C. Davila, M. de Moura, Numerical simulation of mixed-mode progressive delamination in composite materials, Compos. Mater. 37 (2003), doi:10.1177/002199803034505.
[41] A. Turon, P.P. Camanho, J. Costa, C.G. Dávila, A damage model for the simulation of delamination in advanced composites under variable-mode loading, Mech. Mater. 38 (11) (2006) 1072–1089, doi:10.1016/j.mechmat.2005.10.003.